THE JOURNAL OF PHYSICAL CHEMISTRY B

ARTICLE

pubs.acs.org/JPCB

Unusually High Dispersion of Nitrogen-Doped Carbon Nanotubes in DNA Solution

Jin Hee Kim,[†] Masakazu Kataoka,[†] Kazunori Fujisawa,[†] Tomohiro Tojo,[†] Hiroyuki Muramatsu,[‡] Sofía M. Vega-Díaz,[§] F. Tristán-López,[§] Takuya Hayashi,[†] Yoong Ahm Kim,[*,†] Morinobu Endo,[†,‡,§] Mauricio Terrones,[§,∥] and Mildred S. Dresselhaus[*,⊥]

[†]Faculty of Engineering, Shinshu University, 4-17-1 Wakasato, Nagano-shi 380-853, Japan

[‡]Institute of Carbon Science and Technology, Shinshu University, 4-17-1 Wakasato, Nagano 380-8553, Japan

[§]Research Center for Exotic Nanocarbons (JST), Shinshu University, Wakasato 4-17-1, Nagano 380-8553, Japan

[∥]Department of Physics, Department of Materials Science & Materials Research Institute, The Pennsylvania State University, University Park, Pennsylvania 16802-6300, United States

[⊥]Department of Electrical Engineering and Computer Science and Department of Physics, Massachusetts Institute of Technology, Cambridge, Massachusetts 02139-4307, United States

Supporting Information

ABSTRACT: The dispersibility in a DNA solution of bundled multiwalled carbon nanotubes (MWCNTs), having different chemical functional groups on the CNT sidewall, was investigated by optical spectroscopy. We observed that the dispersibility of nitrogen (N)-doped MWCNTs was significantly higher than that of pure MWCNTs and MWCNTs synthesized in the presence of ethanol. This result is supported by the larger amount of adsorbed DNA on N-doped MWCNTs, as well as by the higher binding energy established between nucleobases and the N-doped CNTs. Pure MWCNTs are dispersed in DNA solution via van der Waals and hydrophobic interactions; in contrast, the nitrogenated sites within N-doped MWCNTs provided additional sites for interactions that are important to disperse nanotubes in DNA solutions.

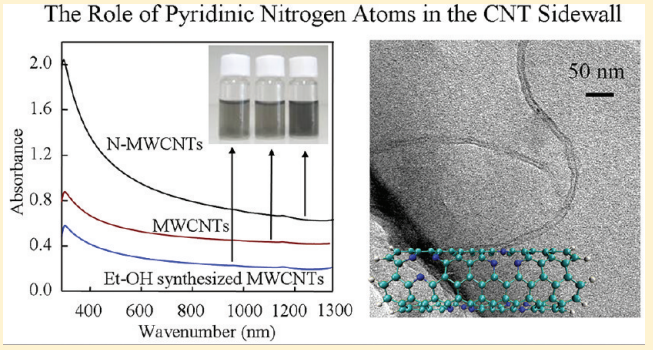

1. INTRODUCTION

Carbon nanotubes (CNTs) can be viewed as graphene that has been rolled into a cylinder with a nanoscale diameter.[1] The excellent mechanical and electrical properties of CNTs and their flexibility make them potentially useful in a wide variety of applications.[2,3] At present, several hundred tons of CNTs are commercially produced each year. However, most of these CNTs are in a strongly bundled state due to the strong van der Waals interactions established between adjacent CNTs. For this reason, improving the processability of CNTs via dispersion (i.e., individualization) is of great importance in order to fully exploit their intrinsic physical and chemical properties at the molecular level. The uniform dispersion of individual CNTs without a marked change in either their length or crystallinity remains a critical challenge in CNT processing. In fact, the conversion rate from noncovalently bundled CNTs to individual CNTs, when using strong sonication and subsequent ultracentrifugation, is quite low. Among the many types of surfactants, DNA, a flexible amphiphilic biopolymer, has been found to be well-suited for dispersing and sorting CNTs.[4−7] Theoretical and experimental studies have found that the van der Waals interactions between the nucleobase backbone of DNA and the hydrophobic CNT sidewall are the main driving force behind the dispersion of CNTs in DNA solution, where DNA is helically wrapped around the CNT sidewall.[8−17] Possible applications of such a hybrid DNA/CNT system have been examined, including biosensors,[18,19] DNA transporters,[20] and field-effect transistors;[21] in these applications, the reproducibility of the hybrid DNA/CNT structure is essential. From the viewpoint of tube crystallinity, intrinsic structural defects in CNTs have been reported to provide an additional driving force behind the dispersion of CNTs in DNA solution.[22] In other words, the surface properties of the CNT sidewall govern the DNA/CNT interaction. Functional groups covalently attached to the sidewall of CNTs are sometimes the byproduct of

Special Issue: H. Eugene Stanley Festschrift

Received: June 8, 2011
Revised: September 7, 2011
Published: October 19, 2011

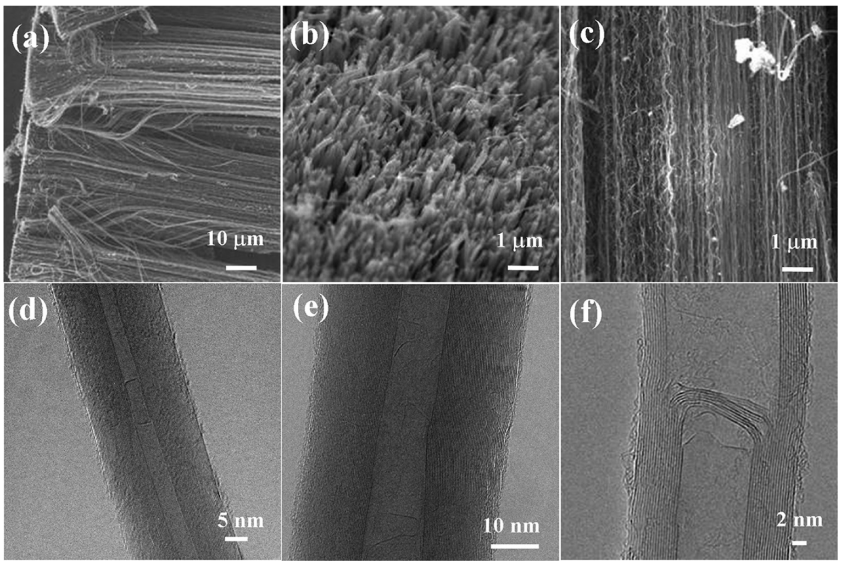

Figure 1. (a−c) Typical SEM images of vertically aligned MWCNTs at different angles and representative TEM images of (d) pure, (e) Et−OH-synthesized, and (f) N-doped MWCNTs.

oxidative purification and could also be intentionally introduced in order to extend the sidewall reactivity.[23−25] However, the role of functional groups in the dispersibility of strongly bundled CNTs still remains an open issue.

In this study, we investigate the role of sidewall functional groups in dispersing three different types of the strongly bundled MWCNTs containing different types of functional groups (e.g., nitrogenated (N) and hydroxyl groups (OH)) in DNA solutions. We note that N-doped MWCNTs exhibited the highest dispersibility in DNA solution, higher than MWCNTs not intentionally doped. Using theoretical calculations, this experimental result was explained by the presence of pyridinic-like nitrogen situated next to carbon vacancies within N-doped MWCNTs, thus contributing to increased binding forces, and a small HOMO−LUMO gap established between the nucleobases and the sidewall of N-doped MWCNTs.

2. EXPERIMENTAL SECTION

We synthesized three different types of MWCNTs by aerosol-assisted chemical vapor deposition. The pure MWCNTs were synthesized by the thermal decomposition of a mixture of 2.5 wt % ferrocene and toluene at 825 °C in an argon atmosphere for 30 min.[26,27] N-doped MWCNTs were obtained by the decomposition of a solution containing 2.5 wt % ferrocene and benzylamine.[28] Finally, highly crystalline MWCNTs (Et−OH synthesized) were produced by using a solution of 2.5 wt % ferrocene, 1 wt % ethanol, and toluene.[29] The three different types of CNTs tested in this work were used without any chemical modification. Subsequently, we prepared an aqueous solution of single-stranded DNA using herring sperm DNA (degraded free acid, Nacalai Tesque Inc.). First, in order to obtain shortened DNA segments with 200 base pairs, we dissolved 10 mg of herring sperm DNA in 10 mL of distilled water under mild sonication (Kubota UP50H, 75%) for 5 min, and then added 1 mL of 1 N sodium hydroxide solution and incubated the solution for 5 min. The DNA solution was neutralized by adding 1 mL of 1 N hydrochloric acid, and then, the DNA solution was stabilized by adding 2 mL of 1 M Tris−HCl buffer solution (pH 8). Then, 10 mg of MWCNT sample (pure, N-doped, or OH-decorated) was dispersed in DNA stock solution under sonication for 1 h at 4 °C. The resultant MWCNT suspensions were placed in an ultracentrifuge (15000*g*) for 1 h in order to remove insoluble material; well-dispersed MWCNT emulsions were thus obtained. The molecular weights of ssDNA before and after sonication are over 20 kb and around 200 bp, respectively. We found a saturated fragmentation of the DNA under our sonication conditions. Indeed, agarose gel electrophoresis of the ssDNA sample showed no additional DNA fragmentation.

With the help of a Qubit fluorometer (Invitrogen), the amount of adsorbed DNA in the MWCNT suspension was measured as follows. First, 5 mL of MWCNT suspension was filtered (0.22 μm) in order to remove free DNA. The remaining materials were redispersed in 5 mL of distilled water using a bath-type sonicator and then the MWCNT suspension was diluted by adding 50 mL of distilled water. Second, we made the working solution by diluting the ssDNA reagent 1:200 in a ssDNA buffer. Next, we added each of the samples to the assay containing the working solution and mixed them together by vortexing them for 2−3 s and we incubated all the tubes at room temperature for 2 min. After calibration using two standard samples, we have recorded the values by inserting the three tubes containing MWCNT suspensions into the Qubit fluorometer. Using UV−vis absorption spectroscopy (Solidspec-3700, Shimadzu), we evaluated the degree of dispersion that was achieved for these three emulsions. We have confirmed the reproducibility of the dispersion state of the MWCNT suspensions by carrying out the same experimental procedure three times. In order to calculate the amount of MWCNT with respect to the amount of DNA, solid-state DNA/MWCNT samples that were prepared by freeze-drying the suspensions were then heated to 700 °C in air on a thermogravimetric analyzer (PerkinElmer, USA). The morphology and the texture of the DNA/MWCNT samples were then observed by field-emission scanning electron microscopy (FE-SEM; JSM6335Fs) and transmission electron microscopy (TEM; JEM-2100F, JEOL). Finally, models of CNTs with different functionalities

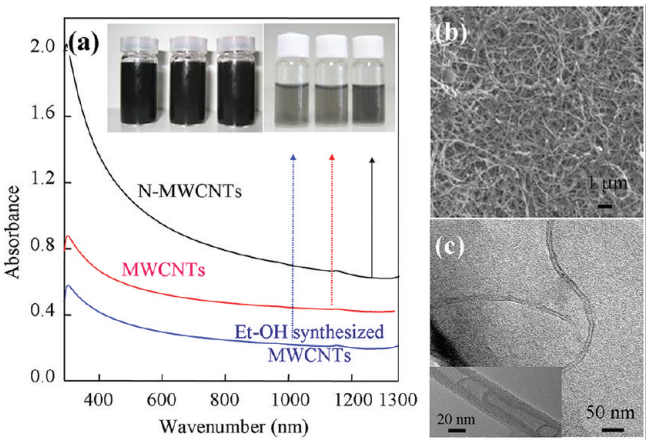

Figure 2. (a) UV absorption spectra of DNA-dispersed pure, Et−OH synthesized, and N-doped MWCNT suspensions (insets: photographs of DNA-dispersed MWCNT suspensions under sonication and after centrifugation). (b) SEM and (c) TEM images of DNA-adsorbed N-doped MWCNTs (inset: high resolution TEM image indicating that the sidewall is fully covered with DNA).

were prepared and optimized using the HyperChem Professional 7.01 program package.[30] Semiempirical molecular orbital theory[31] was used to calculate the binding energy between the four types of nucleobases and the three types of MWCNTs.

3. RESULTS AND DISCUSSION

In this study, we used pure, N-doped, and Et−OH synthesized MWCNT samples, which were grown by aerosol-assisted chemical vapor deposition.[26−29] All the as-prepared samples consisted of MWCNT bundles (Figure 1a), in which the CNTs were aligned along the tube length direction (Figure 1c); after scratching the bundles from the walls of the quartz reactor, we noted that in some cases the tube ends were opened (Figure 1b). No large differences were observed in the degree of crystallinity and the diameter distribution between the three samples (Figure 1d−f), except that for the N-doped and Et−OH synthesized MWNTs the tubular structures were compartmentalized. These as-produced MWCNTs were selected in order to examine the effect of the sidewall functional groups for the following reasons: (1) Even though post-treatments (e.g., strong acids and oxygen plasma) could be used to introduce functional groups to the CNTs, such treatments result in the partial disintegration of the bundled structure and the shortening of the tubes.[23] (2) Two factors that affect the adsorption of DNA on the sidewalls of CNTs are the overall coverage of DNA (which relates to the CNT diameter) and the crystallinity of the CNTs (which relates to the relative number of defects). Experimentally, it is not possible to control both the adsorption of DNA and the crystallinity of the CNTs when using any post-treatment. It is noteworthy that pristine and doped chemical-vapor-deposition-grown MWCNTs were selected because they exhibited similar bundled structures and degrees of crystallinity but had different functional groups on their surface. The basic morphological features of the three types of MWCNTs are summarized in Table SI of the Supporting Information.

We prepared DNA-dispersed MWCNT suspensions by subjecting DNA solutions containing the three MWCNT samples to strong sonication, followed by centrifugation. All three MWCNT

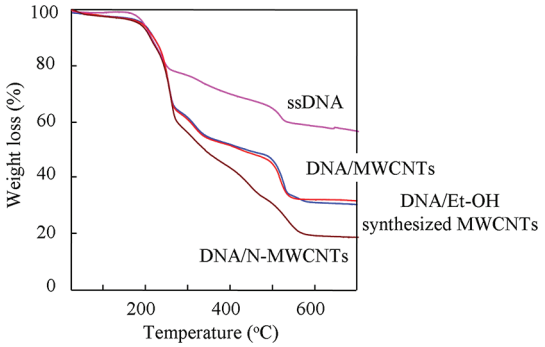

Figure 3. Thermogravimetric profiles, measured in air, of DNA, pure MWCNT/DNA, OH-MWCNTs/DNA, and N-MWCNTs/DNA samples.

suspensions prepared in this way were opaque (Figure 2a, top-left inset), and thus, it was not possible to observe any differences by the naked eye. Upon mild centrifugation, we observed a visual difference between the supernatant obtained from the three MWCNT suspensions: the N-doped MWCNT suspension was more opaque than the pure and Et−OH-synthesized MWCNT suspensions (Figure 2a, top-right inset). With regard to morphology, we observed that the CNTs were randomly and individually dispersed with the aid of DNA (Figure 2b,c), which was thickly coated along the sidewall of individual tubes (inset in Figure 2c), as observed by SEM and TEM. These results indicate a strong interaction between DNA and the sidewall of N-doped tubes. In addition, the absence of structural degradation of the tubes in the dispersion process by a strong sonication was confirmed using Raman studies (see Figure SI, Supporting Information). In order to examine the dispersibility of the three MWCNTs in DNA solution quantitatively, UV−vis absorption spectra were acquired for the three MWCNT suspensions (Figure 2a), because the relative absorbance is proportional to the dispersed amount of CNTs in suspension according to the Lambert−Beer law. When compared with pure and Et−OH-synthesized MWCNTs, N-doped MWCNTs exhibited a 2-fold higher absorbance. However, it is suggested that the presence of bundles in the solution causes an increase in the absorbance background. However, in the case of multiwalled carbon nanotubes, the bundling is less common for the weaker van der Waals forces caused by the presence of imperfect MWNTs. In addition, we have verified the presence of individualized MWCNTs using TEM and SEM observations. Therefore, the increase in the absorbance is not coming from the bundled tubes but rather from the higher amount of the individually dispersed MWCNTs in DNA solution.

In addition, by using a Qubit fluorometer, we measured the ratio of adsorbed DNA to MWCNT in the suspensions by removing any free DNA. The amount of the adsorbed single stranded DNA on carbon nanotubes was found to be 10.1 μg/mL for pure MWCNTs, 10.3 μg/mL for Et−OH-synthesized MWCNTs, and 12.0 μg/mL for N-doped MWCNTs, respectively. This result is also consistent with the higher dispersion of N-doped MWCNTs in a DNA solution.

In addition, in order to measure the dispersed amount of MWCNTs in suspension, thermogravimetric analysis (TGA) was carried out on freeze-dried DNA/MWCNTs in air (Figure 3). Here, we observe that the DNA molecules begin to show an abrupt weight loss in the temperature range 200−300 °C, and

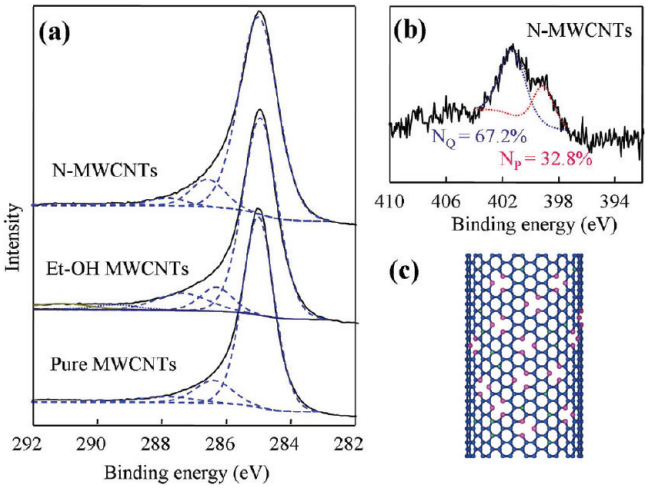

Figure 4. (a) C 1s XPS spectra of pure, Et−OH synthesized, and N-doped MWCNTs. (b) N 1s XPS spectrum of N-doped MWCNTs. (c) A schematic model of N-doped CNTs containing two types of nitrogen atoms.

their yield at 700 °C was found to be about 59%. Both pure MWCNT/DNA and Et−OH-synthesized MWCNT/DNA samples exhibited very similar behaviors, and their yields were both 33%. In contrast, the yield of the DNA/N-MWCNT sample was 20%. However, the pure MWCNT sample was completely burned out. Thus, the amount of carbon nanotubes could be calculated by subtracting the weight loss of the pure DNA from the weight loss of the DNA-wrapped nanotube sample. Such a marked difference in the yield of DNA/MWCNTs and Et−OH-synthesized MWCNTs from that of DNA/N-MWCNTs could be attributed to the larger amount of the dispersed N-MWCNTs in the DNA solution. Nitrogen atoms in CNTs are known to function as anchoring sites for growing metal particles.[32−35] Furthermore, N-doped MWCNTs have been used in a metal-free electrode that has higher electrocatalytic activity, longer-term operation stability, and a greater tolerance to the crossover effect than a platinum electrode for oxygen reduction in an alkaline fuel cell.[36] Moreover, nitrogen atoms are known to improve the biocompatibility of CNTs[37] and a small amount of nitrogen doping (substitutional type) in CNTs could induce metallic behavior.[38]

Such an enhanced performance of N-MWCNTs could be explained by the configuration of the nitrogen atom. To show such effects, we analyzed the bonding nature of carbon and nitrogen atoms in N-MWCNTs by X-ray photoemission spectroscopy (XPS, Figure 4). In all cases, we observed a strong but asymmetric C 1s spectrum. A strong peak at 285.5 eV can be assigned to sp^2-bonded carbon atoms, while a broad peak at 287 eV can be assigned to O−C bonds (Figure 4a). Interestingly, the small, broad peak at 287 eV is here explained by randomly incorporated nitrogen atoms and a net change in the C−N binding energy.[39] In the N 1s XPS spectrum (Figure 4b), we found two configurations of nitrogen atoms in N-MWCNTs: a strong peak at 400.7 eV (N_Q) from substitutional quaternary nitrogen and a relatively weak peak at 398.6 eV (N_P) from pyridinic nitrogen. The amounts of pyridinic and quaternary nitrogens were found to be 32.8 and 67.2%, respectively. When considering the chemical reactivity of the two types of nitrogen atoms, the pyridinic nitrogen atoms exhibit higher activity than

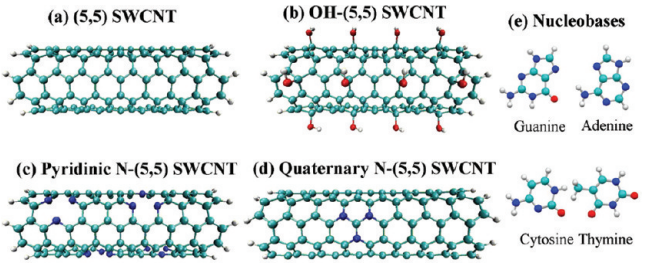

Figure 5. Models of (a) pure, (b) OH-decorated, (c) pyridinic, and (d) quaternary N-doped (5, 5) SWCNTs and (e) the four types of nucleobases.

the substitutional nitrogen atoms because they are positioned next to atomic vacancies (see Figure 4c). From these results, the electron-accepting pyridinic-type nitrogen atoms in CNTs are expected to increase the dispersibility of the CNTs in DNA solution. In this context, theoretical calculations have indicated that van der Waals interactions in N-doped MWNTs are significantly weaker and therefore these doped tubes are more easily dispersible.[40,41]

In order to verify this experimentally observed high dispersibility of N-MWCNTs in aqueous DNA solution, binding-energy calculations on DNA/CNT were carried out by placing four types of nucleobases on pure (5, 5) single-walled CNT (SWCNTs), and on OH-, pyridinic and quaternary N-doped SWCNTs. A pure (5, 5) SWCNT model was prepared by terminating both ends of the SWCNT with hydrogen atoms. The OH-decorated SWCNT model was constructed by covalently attaching OH to the sidewall of the (5, 5) SWCNT, and pyridinic and quaternary nitrogen atoms were incorporated into the SWCNT sidewall (Figure 5a−d). We used the PM6 method to optimize and calculate the energies.[31,40] Subsequently, by placing nucleobases on the sidewall of pure, OH-, pyridinic, and quaternary N-doped SWCNTs (Figure 5e) and after optimizing the atomic structures in order to minimize the total energy of the system, the binding energies (E) (Table 1) were obtained by subtracting the energy of the isolated nucleobases (E_{NB}) and of the SWCNTs (E_{CNT}) from the energy of the combined system (E_{CNT-NB}). The binding energy between the nucleobases and the pure SWCNT model was quite low, with interactions having magnitudes G > T > C ≈ A (weak interactions) for the various nucleobases. However, greatly enhanced binding energies were observed for the pyridinic and quaternary N-doped SWCNTs, and the order of the binding energies then changed to C > T > G > A (strong interactions). The lowest binding energy for the pure SWCNTs and the nucleobases can be explained by the fact that the net change in the dipole moment is small. However, the largest binding energy for N-doped SWCNTs is due to a large change in the dipole moment.

We found that the order of the HOMO−LUMO gap for the three models followed exactly the same order as the binding energies. Notably, the value of the HOMO−LUMO gap for the pyridinic N-doped SWCNT was extremely small (0.126 eV). When calculating the chemical reactivity of the different types of SWCNTs toward nucleobases from the energy gap observed between the LUMO of the nucleobases and the HOMO of the SWCNTs (where nucleobases are acceptors and SWCNTs are donors), the ease of the surface adsorption of nucleobases onto the pyridinic N-doped SWCNT was found to be the highest. According to these theoretical calculations, adenine, when

Table 1. Theoretically Calculated Binding Energy, Dipole Moment, and HOMO−LUMO Gap for Pure, OH-Decorated, and Pyridinic and Quaternary N-Doped (5, 5) SWCNT with Various Nucleobases

sample I.D.		adenine	cytosine	guanine	thymine
pure SW CNT	binding energy[a]	−0.0874	−0.0969	−0.2382	−0.1698
	dipole moment	0.158	0.180	0.114	0.002
	HOMO−LUMO gap	7.033	7.125	6.959	6.899
OH-SWCNT	binding energy[a]	−0.6099	−0.8222	−0.9204	−0.8699
	dipole moment	0.093	2.967	3.244	4.184
	HOMO−LUMO gap	6.716	6.809	6.642	6.582
pyridinic N-SWCNT	binding energy[a]	−1.3221	−2.7018	−2.0682	−2.4275
	dipole moment	0.922	6.811	2.309	1.699
	HOMO−LUMO gap	0.026	0.067	0.100	0.160
quaternary N-SWCNT	binding energy[a]	−0.5961	−1.8499	−0.7528	−1.0583
	dipole moment	6.736	16.7	9.275	14.887
	HOMO−LUMO gap	0.041	0.052	0.115	0.175

[a] Binding energies (E) were obtained by subtracting the energy of the isolated nucleobase (E_{NB}) and of the CNT (E_{CNT}) from the energy of the combined system ($E_{CNT} - N_{NB}$).

adsorbed on the SWCNT, induces a small change in the dipole moment, thus resulting in a weak interaction with the CNT sidewall. In contrast, DNA which contains a large fraction of cytosine is expected to improve the dispersibility of CNTs.

4. CONCLUSIONS

Here, we have presented both experimental and theoretical evidence demonstrating that the dispersibility of MWCNTs in DNA solution strongly depends on the type of functional group that is attached to the CNT sidewall. The particularly high dispersion of N-doped MWCNTs in DNA solutions, when compared with that of pure and Et−OH-synthesized MWCNTs, is explained by the presence of nitrogenated sites (substitutional and pyridinic) present on the CNT sidewall. DNA molecules could readily adsorb onto the hydrophobic surface of the pure CNT via $\pi-\pi$ stacking interactions. On the basis of our theoretical calculations, a pyridinic nitrogen next to carbon vacancies in N-doped MWCNTs was found to be a major contributor to the large binding energy, as well as to the small HOMO−LUMO gap between the nucleobases and the sidewall of N-doped MWCNTs. The calculations also revealed that DNA which contains a large fraction of cytosine could significantly improve the dispersibility of both SWCNTs and MWCNTs.

■ ASSOCIATED CONTENT

Supporting Information. The basic features of the three types of multiwalled carbon nanotubes are summarized in Table SI. Raman spectra of DNA-dispersed MWCNT samples are shown in Figure SI. This material is available free of charge via the Internet at http://pubs.acs.org.

■ AUTHOR INFORMATION

Corresponding Author

*Phone: +81-26-269-5210 (Y.A.K.); +1-617-253-6864 (M.S.D.). Fax: +81-26-269-5208 (Y.A.K.); +1-617-253-6827 (M.S.D.). E-mail: yak@endomoribu.shinshu-u.ac.jp+81-26-269-5208 (Y.A.K.); millie@mgm.mit.edu (M.S.D.).

■ ACKNOWLEDGMENT

We acknowledge the support from the Regional Innovation Cluster Program of Nagano from the Ministry of Education, Culture, Sports, Science and Technology of Japan. J.H.K. acknowledges the support of Shinshu University Global COE Program "International Center of Excellence on Fiber Engineering". M.S.D. acknowledges NSF10-04147. M.T., S.M.V.-D., F.T.-L., and M.E. acknowledge support from the Research Center for Exotic NanoCarbon Project, Japan Regional Innovation Strategy Program by the Excellence, JST.

■ REFERENCES

(1) Dresselhaus, M. S.; Dresselhaus, G.; Eklund, P. *Science of Fullerenes and Carbon Nanotubes*; Academic Press: New York, 1996.

(2) Baughman, R. H.; Zakhidov, A. A.; de Heer, W. A. Carbon Nanotubes—the Route Toward Applications. *Science* **2002**, *297*, 787–792.

(3) Jorio, A.; Dresselhaus, M. S.; Dresselhaus, G. *Carbon Nanotubes: Advanced Topics in the Synthesis, Structure, Properties and Applications*; Springer: New York, 2008.

(4) Nakashima, N.; Okuzono, S.; Murakami, H.; Nakai, T.; Yoshikawa, K. DAN Dissolves Single-walled Carbon Nanotubes in Water. *Chem. Lett.* **2003**, *32*, 456–457.

(5) Zheng, M.; Jagota, A.; Semke, E. D.; Diner, B. A.; McLean, R. S.; Lustig, S. R.; Richardson, R. E.; Tassi, N. G. DNA-assisted dispersion and separation of carbon nanotubes. *Nat. Mater.* **2003**, *2*, 338–342.

(6) Zheng, M.; Jagota, A.; Strano, M. S.; Santos, A. P.; Barone, P.; Chou, S. G.; Diner, B. A.; Dresselhaus, M. S.; Mclean, R. S.; Onoa, G. B.; Samsonidze, G. G.; Semke, E. D.; Usrey, M.; Walls, D. J. Structure-Based Carbon Nanotube Sorting by Sequence-Dependent DNA Assembly. *Science* **2003**, *302*, 1545–1548.

(7) Kim, J. H.; Kataoka, M.; Kim, Y. A.; Shimamoto, D.; Muramatsu, H.; Hayashi, T.; Endo, M.; Terrones, M.; Dresselhaus, M. S. Diameter-Selective Separation of Double-Walled Carbon Nanotubes. *Appl. Phys. Lett.* **2008**, *93*, 223107.

(8) Strano, M. S.; Zheng, M.; Jagota, A.; Onoa, G. B.; Heller, D. A.; Barone, P. W.; Usrey, M. L. Understanding the Nature of the DNA-Assisted Separation of Single-Walled Carbon Nanotubes Using Fluorescence and Raman Spectroscopy. *Nano Lett.* **2004**, *4*, 543–550.

(9) Zheng, M.; Diner, B. A. Solution Redox Chemistry of Carbon Nanotubes. *J. Am. Chem. Soc.* **2004**, *126*, 15490–15494.

(10) Fantini, C.; Jorio, A.; Santos, A. P.; Peressinotto, V. S. T.; Pimenta, M. A. Characterization of DNA-Wrapped Carbon Nanotubes

by Resonance Raman and Optical Absorption Spectroscopies. *Chem. Phys. Lett.* **2007**, *439*, 138–142.

(11) Zhao, X.; Johnson, J. K. Simulation of Adsorption of DNA on Carbon Nanotubes. *J. Am. Chem. Soc.* **2007**, *129*, 10438–10445.

(12) Meng, S.; Maragakis, P.; Papaloukas, C.; Kaxiras, E. DNA Nucleoside Interaction and Identification with Carbon Nanotubes. *Nano Lett.* **2007**, *7*, 45–50.

(13) Chen, Y.; Liu, H.; Ye, T.; Kim, J.; Mao, C. DNA-Directed Assembly of Single-Wall Carbon Nanotubes. *J. Am. Chem. Soc.* **2007**, *129*, 8696–8697.

(14) Vogel, S. R.; Kappes, M. M.; Hennrich, F.; Richert, C. An Unexpected New Optimum in the Structure Space of DNA Solubilizing Single-Walled Carbon Nanotubes. *Chem.—Eur. J.* **2007**, *13*, 1815–1820.

(15) Das, D.; Sood, A. K.; Maiti, P. K.; Das, M.; Varadarajan, R.; Rao, C. N. R. Binding of Nucleobases with Single-Walled Carbon Nanotubes: Theory and experiment. *Chem. Phys. Lett.* **2008**, *453*, 266–273.

(16) Carot, M. L.; Torresi, R. M.; Garcia, C. D.; Esplandiu, M. J.; Giacomelli, C. E. Electrostatic and Hydrophobic Interactions Involved in CNT Biofunctionalization with Short ss-DNA. *J. Phys. Chem. C* **2010**, *114*, 4459–4465.

(17) Kim, J. H.; Kataoka, M.; Shimamoto, D.; Muramatsu, H.; Jung, Y. C.; Hayashi, T.; Kim, Y. A.; Endo, M.; Park, J. S.; Saito, R.; Terrones, M.; Dresselhaus, M. S. Raman and Fluorescence Spectroscopic Studies of a DNA-Dispersed Double Walled Carbon Nanotube Solution. *ACS Nano* **2010**, *4*, 1060–1066.

(18) Staii, C.; Johnson, A. T.; Chen, M.; Gelperin, A. DNA-Decorated Carbon Nanotubes for Chemical Sensing. *Nano Lett.* **2005**, *5*, 1774–1778.

(19) Gao, H.; Kong, Y. Simulation of DNA-Nanotube Interactions. *Annu. Rev. Mater. Res.* **2004**, *34*, 123–150.

(20) Kam, N. W. S.; Liu, Z.; Dai, H. Carbon Nanotubes as Intracellular Transporters for Proteins and DNA: An Investigation of the Uptake Mechanism and Pathway. *Angew. Chem., Int. Ed.* **2006**, *45*, 577–581.

(21) Lu, Y.; Bangsaruntip, S.; Wang, X.; Zhang, L.; Nishi, Y.; Dai, H. DNA Functionalization of Carbon Nanotubes for Ultrathin Atomic Layer Deposition of High K Dielectrics for Nanotube Transistors with 60 mV/Decade Switching. *J. Am. Chem. Soc.* **2006**, *128*, 3518–3519.

(22) Kim, J. H.; Kataoka, M.; Shimamoto, D.; Muramatsu, H.; Jung, Y. C.; Tojo, T.; Hayashi, T.; Kim, Y. A.; Endo, M.; Terrones, M.; Dresselhaus, M. S. Defect-enhanced Dispersion of Carbon Nanotubes in DNA Solutions. *ChemPhysChem* **2009**, *10*, 2414–2417.

(23) Liu, J.; Rinzler, A. G.; Dai, H. J.; Hafner, J. H.; Bradley, R. K.; Boul, P. J.; Lu, A.; Iverson, T.; Shelimov, K.; Huffman, C. B.; Rodriguez-Macias, F.; Shon, Y. S.; Lee, T. R.; Colbert, D. T.; Smalley, R. E. Fullerene Pipes. *Science* **1998**, *280*, 1253–1256.

(24) Ivanov, V.; Fonseca, A.; Nagy, J. B.; Lucas, A.; Lambin, P.; Bernaerts, D.; Zhang, X. B. Catalytic Production and Purification of Nanotubules Having Fullerene-Scale Diameters. *Carbon* **1995**, *33*, 1727–1738.

(25) Wong, S. S.; Joselevich, E.; Woolley, A. T.; Cheung, C. L.; Lieber, C. M. Covalently Functionalized Nanotubes as Nanometre-Sized Probes in Chemistry and Biology. *Nature* **1998**, *394*, 52–55.

(26) Kamalakaran, R.; Terrones, M.; Seeger, T.; Kohler-Redlich, Ph.; Ruhle, M.; Kim, Y. A.; Hayashi, T.; Endo, M. Synthesis of Thick and Crystalline Nanotube Arrays by Spray Pyrolysis. *Appl. Phys. Lett.* **2000**, *77*, 3385–3387.

(27) Mayne, M.; Grobert, N.; Terrones, M.; Kamalakaran, R.; Rhle, M.; Kroto, H. W.; Walton, D. R. M. Pyrolytic Production of Aligned Carbon Nanotubes from Homogeneously Dispersed Benzene-Based Aerosols. *Chem. Phys. Lett.* **2001**, *338*, 101–107.

(28) Terrones, M.; Ajayan, P. M.; Banhart, F.; Blase, X.; Carroll, D. L.; Charlier, J. C.; Czerw, R.; Foley, B.; Grobert, N.; Kamalakaran, R.; Kohler-Redlich, P.; Rühle, M.; Seeger, T.; Terrones, H. N-Doping and Coalescence of Carbon Nanotubes: Synthesis and Electronic properties. *Appl. Phys. A: Mater. Sci. Process.* **2002**, *74*, 355–361.

(29) Botello-Mendez, A. R.; Campos-Delgado, J.; Morelos-Gmez, A.; Romo-Herrera, J. M.; Rodrguez, A. G.; Navarro, H.; Vidal, M. A.; Terrones, H.; Terrones, M. Controlling the Dimensions, Reactivity and Crystallinity of Multiwalled Carbon Nanotubes using Low Ethanol Concentrations. *Chem. Phys. Lett.* **2008**, *453*, 55–61.

(30) Ivanciuc, O. HyperChem Release 4.5 for Windows. *Chem. Inf. Comput. Sci.* **1996**, *36*, 612–614.

(31) Stewart, J. J. P. Optimization of parameters for semiempirical methods V: Modification of NDDO approximations and application to 70 elements. *J. Mol. Model.* **2007**, *13*, 1173–1213.

(32) Jiang, K.; Schadler, L. S.; Siegel, R. W.; Zhang, X. J.; Zhang, H. F.; Terrones, M. Protein Immobilization on Carbon Nanotubes via a Two-Step Process of Diimide-Activated Amidation. *J. Mater. Chem.* **2004**, *14*, 37–39.

(33) Jiang, K.; Eitan, A.; Schadler, L. S.; Ajayan, P. M.; Siegel, R. W.; Grobert, N.; Mayne, M.; Reyes-Reyes, M.; Terrones, H.; Terrones, M. Selective Attachment of Gold Nanoparticles to Nitrogen-Doped Carbon Nanotubes. *Nano Lett.* **2003**, *3*, 275–277.

(34) Zamudio, A.; Elias, A. L.; Rodriguez-Manzo, J. A.; Lopez-Urias, F.; Rodriguez-Gattorno, G.; Lupo, F.; Ruhle, M.; Smith, D. J.; Terrones, H.; Diaz, D.; Terrones, M. Efficient Anchoring of Silver Nanoparticles on N-Doped Carbon Nanotubes. *Small* **2005**, *2*, 346–350.

(35) Lepro, X.; Vega-Cantu, Y.; Rodriguez-Macias, F. J.; Bando, Y.; Golberg, D.; Terrones, M. Production and Characterization of Coaxial Nanotube Junctions and Networks of CN_x/CNT. *Nano Lett.* **2007**, *7*, 2220–2226.

(36) Gong, K.; Du, F.; Xia, Z.; Durstock, M.; Dai, L. Nitrogen-Doped Carbon Nanotube Arrays with High Electrocatalytic Activity for Oxygen Reduction. *Science* **2009**, *323*, 760–764.

(37) Carrero-Sanchez, J. L.; Elias, A. L.; Mancilla, R.; Arellin, G.; Terrones, H.; Laclette, J. P.; Terrones, M. Biocompatibility and Toxicological Studies of Carbon Nanotubes Doped with Nitrogen. *Nano Lett.* **2006**, *6*, 1609–1616.

(38) Golberg, D.; Dorozhkin, P. S.; Bando, Y.; Dong, Z. C.; Tang, C. C.; Uemura, Y.; Grobert, N.; Reyes-Reyes, M.; Terrones, H.; Terrones, M. Structure, Transport and Field-Emission Properties of Compound Nanotubes: $CN_x (x < 0.1)$. *Appl. Phys. A: Mater. Sci. Process.* **2003**, *76*, 499–507.

(39) Ayala, P.; Grüneis, A.; Gemming, T.; Grimm, D.; Kramberger, C.; Ru1mmeli, M. H.; Freire, F. L., Jr.; Kuzmany, H.; Pfeiffer, R.; Barreiro, A.; Bu1chner, B.; Pichler, T. Tailoring N-Doped Single and Double Wall Carbon Nanotubes from a Nondiluted Carbon/Nitrogen Feedstock. *J. Phys. Chem. C* **2007**, *111*, 2879–2884.

(40) Sumpter, B. G.; Huang, J. S.; Meunier, V.; Romo-Herrera, J. M.; Cruz-Silva, E.; Terrones, H.; Terrones, M. A Theoretical and Experimental Study On Manipulating the Structure and Properties of Carbon Nanotubes Using Substitutional Dopants. *Int. J. Quantum Chem.* **2009**, *109*, 97–118.

(41) Sumpter, B. G.; Meunier, V.; Romo-Herrera, J. M.; Cruz-Silva, E.; Cullen, D. A.; Terrones, H.; Smith, D. J.; Terrones, M. Nitrogen-Mediated Carbon Nanotube Growth: Diameter Reduction, Metallicity, Bundle Dispersability, and Bamboo-like Structure Formation. *ACS Nano* **2007**, *1*, 369–375.